Solid State Communications 251 (2017) 60–65

Contents lists available at ScienceDirect

Solid State Communications

journal homepage: www.elsevier.com/locate/ssc

Communication

The magnetic vortex gyration mediated by spin-polarized current in a confined off-centered nanocontact structure

Huanan Li, Dongfei Li*, Yaxin Wang, Zhong Hua

College of Physics, Jilin Normal University, Siping 136000, China

ARTICLE INFO

Keywords:
Magnetic vortex core
Confined nanocontact system
Gyrotropic motion
Micromagnetic simulations

ABSTRACT

We study the magnetic vortex dynamical behaviors in a confined off-centered nanocontact system through micromagnetic simulations. It is found that the vortex core could be pinned when the nanocontact is shifted to large enough distance from the center of the nanodisk. We also find that the position of nanocontact exerts great influence on the vortex core gyration, including trajectory, eigenfrequency, excitation time, and instantaneous velocity. The simulations show that it is possible to utilize the nanocontact position to change the total effective potential energy of the system so as to realize both the pinning of the vortex core and the controllability of vortex core gyration. The characteristic gyration in this system is advantageous to control the polarity switching and other dynamical behaviors of magnetic vortex.

1. Introduction

A magnetic vortex stabilized in a micron or submicron sized ferromagnetic structure is a curling magnetization distribution and the magnetization points perpendicularly to the plane with about 10 nm-sized vortex core (VC) at the center of the platelet. The magnetic state could be characterized by the polarity of the VC, pointing up (p=1) or down (p=−1) and by the curling direction of the in-plane magnetization, clockwise (c=−1) or counterclockwise (c=1) [1–3]. Dynamics of magnetic vortex in nanostructures have been studied extensively, in particular, the gyrotropic motion corresponding to lowest frequency mode [4–8]. The gyrotropic motion refers to a displaced VC exhibiting motion with a continuously increasing orbital radius and finally attaining a steady orbit with a constant orbital radius and a characteristic value of eigenfrequency. Recent experimental studies reported that this motion can also be excited by spin-polarized current [9,10]. From then on, the gyration of vortex driven by spin-polarized currents in nanopillars [10–18] and single nanocontact structures [19–26] has attracted intensive attentions because of its potential application characterized by high output power and narrow linewidth in spin-transfer microwave oscillators [27].

In recent years, many studies about the characteristics of VC gyration have been demonstrated. Kasai et al. reported that VC can be resonantly excited by an in-plane ac current and the oscillation frequency can be tuned by the sample shape [28]. Pribiag et al. observed that an out-of-plane spin-polarized dc current-induced oscillation frequency of a magnetic vortex in a nanopillar exhibits much narrower linewidth than uniform nanomagnets [9]. Further studies demonstrated that vortex oscillation can be reliably controlled by current density and direction of current flow [14]or changing the magnetization in the polarizing layer [24,29]. Moreover, Mistral et al. experimentally demonstrated that the VC would attain a stable circular orbit outside of the nanocontact region under the effect of a spin-polarized current [19]. Manfrini et al. found that the oscillation frequency in nanocontact geometry shows good agility and it has potential application in microwave modulation schemes [20]. Furthermore, vortex-antivortex pair rotations were observed for the case of large nanocontact diameter [21,30].

These above-mentioned studies not only provided methods triggering vortex gyration but also demonstrated strategies controlling vortex oscillation. However, both nanopillars and nanocontacts have limitations. In nanopillar geometry, the steady oscillation of VC only occurs within a very small current density range, making application be difficult [12,31,32]. In single nanocontact geometry, the current is injected into a multilayer element via a contact with the diameter about 10–100 nm, has been considered as the most interesting devices [19,22,24]. This is because the steady vortex oscillation can occur in a very large current density range. Nevertheless, the effect of the sample size cannot be considered when designing the associated device, meanwhile, a magnetic field or current with sufficient strength should be applied to create a vortex in the continuous magnetic film. Taking into these factors into consideration, we designed a confined nanocontact system where the current is constrained into a contact region in the nanopillar structure [33]. In such system, we found that

* Corresponding author.
E-mail addresses: jiyonghnli@126.com (H. Li), huazhongnan@126.com (D. Li).

http://dx.doi.org/10.1016/j.ssc.2016.12.015
Received 8 September 2016; Received in revised form 14 November 2016; Accepted 21 December 2016
Available online 21 December 2016

the steady oscillations of vortex can sustain a wider current range, and the oscillation frequency depends on the VC position [33]. However, the VC is difficult to excite if the nanocontact is placed at the center of the sample because of circularly symmetric potential energy, the common solution to solve this problem is to add a biased field to shift the VC before applying the perpendicular spin-polarized current [31,33]. Most recently, we realized the purposes of easier excitation of VC and gaining a nonuniform frequency of the VC steady oscillation through using multinanocontacts in such confined geometry [34,35]. Actually, according to some relevant experimental reports, the nanocontact could be designed flexibly in the sample [36,37], in this paper, we therefore design a very simple model to realize the purposes of easier excitation of VC, steady oscillation within a wider current range, and the controllability of VC gyration. We utilize a single nanocontact geometry, with the nanocontact shifted from the nanodisk center to break the symmetry of the potential energy. Through simulations, we find the VC could be excited as long as the current applied, and its gyration, including trajectory, eigenfrequency, excitation time, and instantaneous velocity on the steady orbits also could be mediated by the nanocontact position. Meanwhile, we find an interesting dynamical phenomenon, namely, the VC could be pinned in the absence of external magnetic field or introducing defects only shifting the nanocontact large enough distance from the disk center.

2. Model and results

As shown in Fig. 1(a), a permalloy (Py: $Ni_{80}Fe_{20}$) nanodisk of diameter $2R$=400 nm and thickness L=10 nm is chosen to be the model system. Its ground state is a magnetic vortex with (p,c)=(1,1). To excite the vortex, an out-of-plane spin-polarized current is injected into the nanodisk through a nanocontact, where the nanocontact does not locate at the center of the nanaodisk but at the y-axis with radius R_c=50 nm and a tunable distance d between the nanocontact and the disk centers. Here we define +z (-z) direction of the applied current as i_p=1(i_p=−1), and the spin polarization direction is assumed to be S_p=−1.

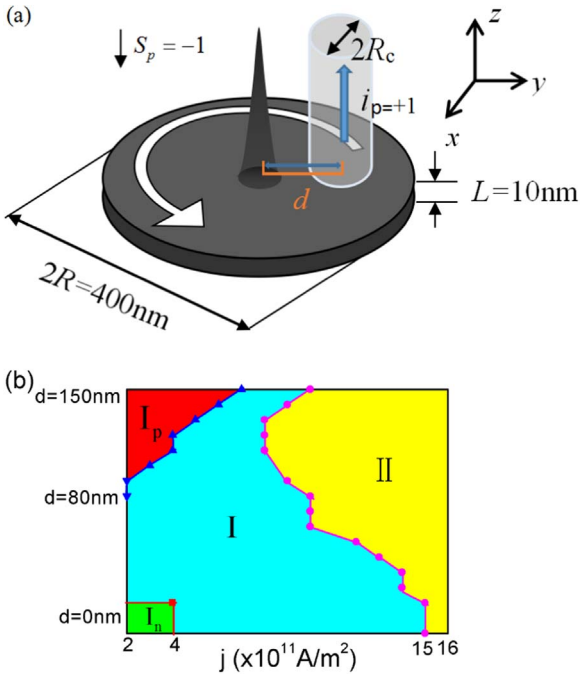

Fig. 1. (Color online) (a) Schematic illustration of an off-centered system. The ground state of the Py nanodisk is vortex with (p, c)=(1,1), which indicates by the out-of-plane cone and white arrow, respectively. Out-of-plane spin-polarized current is applied to the Py nanodisk through a nanocontact represented by white cylinders with radius R_c. The nanocontact lies in the y-axis and its distance to the center of the nanodisk is d. The blue and black arrows represent the direction of applied current and spin polarization. (b) The dynamical behaviors of magnetic vortex with respect to current density j for various d. The color-coded different regions, marked by I_n (green), I_p (red), I (light blue) and II (yellow), represent no VC excitation, VC pinning, VC gyration, and the polarity of VC switching, respectively.

The vortex dynamics are calculated by the Object Oriented Micromagnetic Framework (OOMMF) code, which is based on the Laudau-liftshitz-Gilbert equation extended by the Slonczewski spin-transfer torque [38,39]. To compare the results of the micromagnetic simulations with a real material system, we selected typical parameters for the simulations, including the saturation magnetization M_s=8.6×10^5 A/m, the spin polarization P=0.4, the exchange constant A=1.3×10^{-11} J/m, the Gilbert damping parameter α=0.05, and the unit cell size is 2.5×2.5×10 nm^3. We also did the testing simulations with unit cell 2.5×2.5×2.5 nm^3, and the resulted effect of off-centered structure on the vortex dynamics is the same as that calculated with the 2D square lattice. Therefore, the cell size used in our paper is safe to speed up the computation of vortex dynamics. In this study, both the spin-transfer-torque of spin-polarized current acting directly on vortex and comparable Oersted field accompanying the current are taken into consideration, where the Oersted field is calculated using Biot-Savart's law.

We firstly confirm the complete vortex dynamical phenomena in this system. It is found that the VC exhibits four different dynamical behaviors with current density j ranging from 2 to 16×10^{11}A/m^2 as shown in Fig. 1(b). For d=0 nm, where the nanocontact is placed at the center of the nanodisk, the VC could not be excited when the current density is less than a certain value as shown in regime I_n. When the nanocontact is shifted to a moderate distance (0 < d < 80 nm), we observe that the VC is triggered to gyrotropic motion (regimeI) as long as the current is applied. Whereas, we find an interesting dynamical behavior when the nanocontact is shifted to large enough distance (d≥80 nm), the VC is excited to analogous gyration firstly and quickly it is pinned at some position of the nanodisk as shown in regime I_p. With the increasing current density for each of d, the polarity of VC is switched (regime II). In a word, we observe that the critical current density for VC switching decreases with the increasing d. The VC is excited to gyration for moderate distances, but the VC is pinned at large distances and low current densities. Therefore, the VC dynamical behaviors are controllable by changing the nanocontact position and current density in such geometry.

As the next step, the dynamical behaviors at relative low current density for each of d are explored. The trajectory of the VC for representative d at j=6×10^{11}A/m^2 is summarized in Figs. 2(a)-2(d). Fig. 2(a)-(c) show that the VC experiences spiral motion until reach a steady-state orbit. This means that the steady oscillation of VC can be achieved when d is not so large at relative low current density. However, the VC could not attain the steady oscillation when j is relative low at large d. As shown in Fig. 2(d), the VC could not attain steady oscillation after it is triggered at d=150 nm but be pinned at some position of y-axis of the nanodisk. This new dynamical behavior implies that the VC position is controllable by changing the position of the nanocontact. And such significant dynamical behaviors reveal that the dynamical properties of VC are strongly modified by the nanocontact position, and according to micromagnetics theory, the pinned position of VC should be the position where the total energy is minimum. Then, we should clarify the changes of the total effective potential energy when the nanocontact is shifted. The total effective potential energy includes magnetostatic energy due to the core displacement and Oersted field energy inducing by the applied current (Exchange energy is ignored because it is very low in our model system), and our previous work has demonstrated the detail calculation process of total effective potential energy [40]. The backgrounds of Fig. 2 show the distributions of total effective potential energy for various d. The total energy is circularly symmetric at d=0 nm, leading to the circular orbit and the center of gyration is the center of the

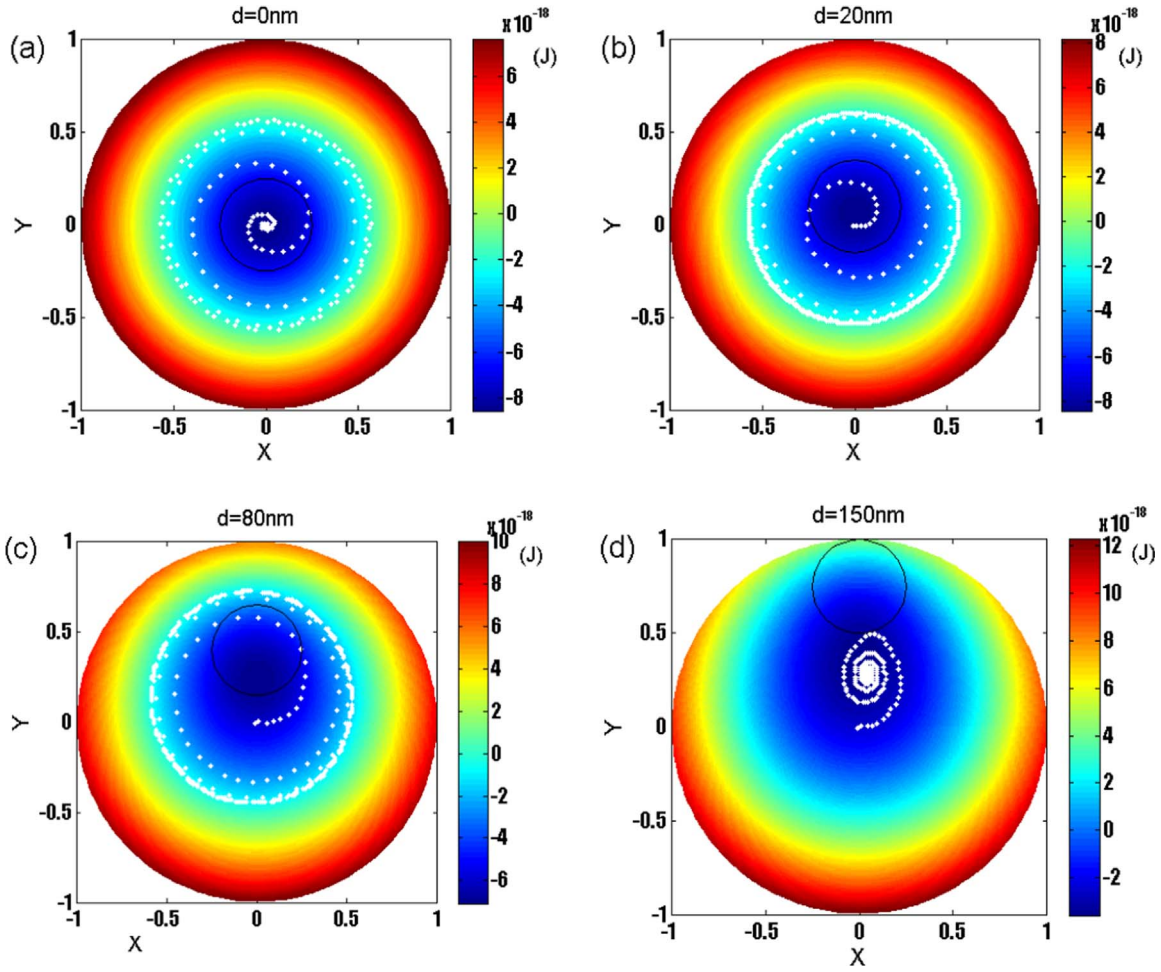

Fig. 2. (Color online) The trajectory of VC (white dots) for (a) d=0 nm, (b) d=20 nm, (c) d=80 nm, (d) d=150 nm at the current density j=6×10^{11} A/m^2. The backgrounds show the contour plots of the total effective potential energy versus the VC position, where the black circle denotes the nanocontact.

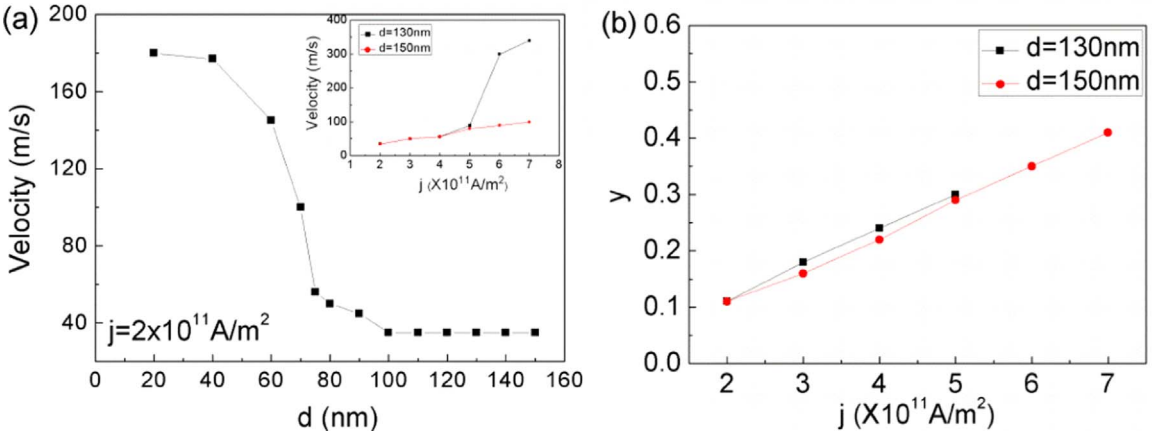

Fig. 3. (a) The maximum excitation velocity as a function of d at the same current density j=2×10^{11} A/m^2. The insert is the maximum excitation velocity as a function of j at d=130 nm and d=150 nm. (b) The pinning position depending on the variation of d and j.

nanodisk. Whereas, the circular symmetry of the total energy is somewhat broken when the nanocontact is shifted from the center of the nanodisk, yielding the equilibrium position is also changed and the changes of equilibrium position result in the center of VC gyration changes but maintaining the steady circular orbit. However, it is obvious that the circular symmetry of total energy is completely broken at d=150 nm, leading to the peculiar dynamical behavior of VC, the VC is excited firstly with very small gyration radius but quickly it is pinned at a position of y-axis. We attribute the non-circular orbit of VC with small gyration radius to the nonuniform distributions of total energy on the nanodisk, the higher energy forces the VC to move with very small radius, and thus it is very close to the energy potential well and be pinned easily. Furthermore, we can analyze the VC pinning behavior from maximum excitation velocity, Fig. 3(a) shows the variation of maximum excitation velocity with d at j=2×10^{11}A/m^2. It is observed that the maximum excitation velocity decreases with the increasing d, which results in the VC is difficult to obtain the steady orbit for larger d. It shows that the VC will be pinned when the velocity decreases to

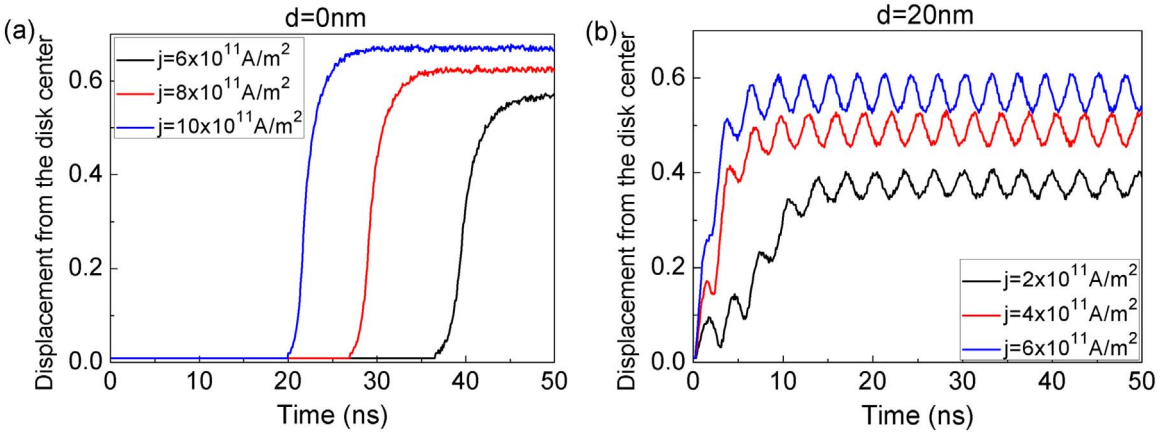

Fig. 4. VC displacement from the disk center as a function of simulation time (a) for d=0 nm (b) for d=20 nm.

50 m/s at d=80 nm. Moreover, the maximum excitation velocity shows almost the same value when j is small, however, velocity increases rapidly with increasing j shown as the insert in Fig. 3(a), thus yielding the VC is easier to obtain the steady gyration for smaller distance. And next, it is necessary to clarify the relation between the pinning position and the distance, and its dependence on the current density. As revealed in Fig. 3(b), the pinning position shows a monotonic function with increasing j and it shows a larger value for smaller d at a fixed j. Therefore, the VC exhibits gyration at smaller d and it will be pinned at larger d. Actually, it is necessary to analyze gyroforce, damping force, restoring force, and spin-transfer force in Thiele equation for further investigations [19,40], we will do further analysis in our future work. It should be pointed out there is another change of vital physical parameter induced by total energy distributions worthy to display, which is the excitation time of the vortex. The excitation time is defined as the time interval between the application of current and the VC departure from the disk center. In order to clarify the differences of excitation time between the case of d=0 and $d\neq0$, we plot the VC displacement from the disk center as a function of simulation time in Fig. 4. Fig. 4(a) shows that the excitation time decreases with increasing current density, the VC takes about 35 ns to deviate from the disk center at d=0 nm and j=6×10^{11}A/m^2 and this value decreases to 20 ns when j=10×10^{11} A/m^2, the circular symmetry of total energy leads to the VC is difficult to be excited. On the contrary, we observe that the VC will depart disk center as long as the current is applied to the disk at $d\neq0$ shown in Fig. 4(b) and the current density refers to $j\geq2\times10^{11}$ A/m^2. This interesting phenomenon implies that the VC could be easier to excite because of the asymmetry of the total effective potential energy, resulting in faster polarity reversal with lower current density [40,41].

Next, we will pay our emphasis on the VC gyration. We first investigate the eigenfrequency of steady oscillation. The eigenfrequency represents the average rotation frequency of VC in one period, which is obtained by performing fast Fourier transformation on the $<m_x>$. Fig. 5(a) shows the dependence of eigenfrequency on d at j=8×10^{11} A/m^2. We observe that the eigenfrequency shows great dependence on d, the eigenfrequency decreases with the increases of d when j is fixed. Moreover, the eigenfrequency is also sensitive to j, which increases with increasing of j at each of d, as shown in Fig. 5(b). The changing trend of eigenfrequency can be explained by the Oersted field. It has shown that the Oersted field influences the gyrotropic frequency, when the curling direction of the field is with the same (opposite) direction as the chirality of the vortex, gyrotropic frequency will increase (decrease) [42]. So the eigenfrequency is maximum at d=0 nm because of the same direction of the Oersted field with vortex chirality. However, with the increasing d, the more discrepancy between the Oersted field and the vortex chirality leads to the less eigenfrequency. Let us look at this problem from another angle, actually, the changes of eigenfrequency also reflect the period of VC gyration on the steady trajectory. The VC needs much more time to complete gyration of one period when d is increased at a fixed j and it needs less time to complete gyration of one period when j is increased.

Another important physical parameter of gyration is instantaneous velocity. Fig. 6(a) and (b) show the VC displacement from the disk center and the velocity of VC gyration as a function of simulation time, respectively. We observe that the displacements also display periodic fluctuation with the increasing d because of equilibrium shifts. Therefore, it is referred that the combined effects of displacements shown in Fig. 6(a) and instantaneous frequency result in the formation of periodic peaks of instantaneous velocity shown in Fig. 6(b). The

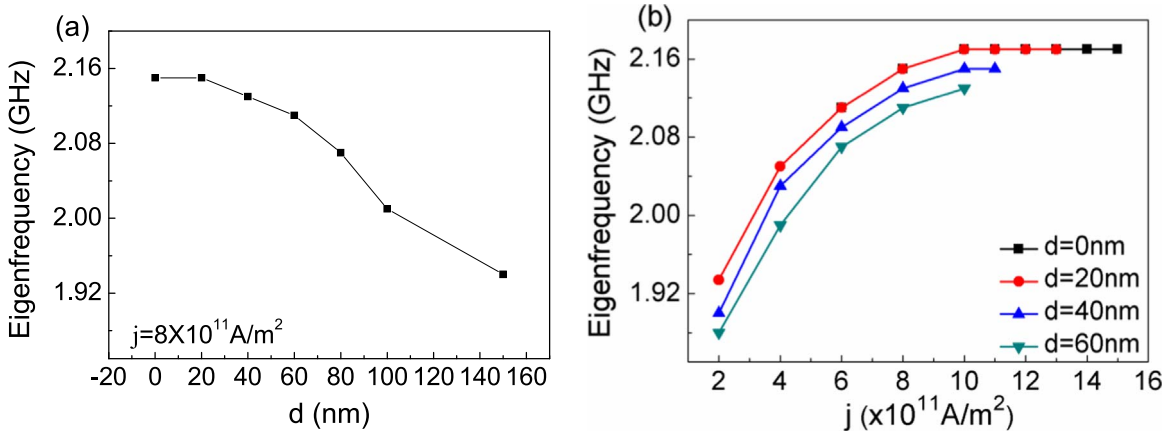

Fig. 5. The eigenfrequency of the VC steady oscillation as a function of (a) d at j=8×10^{11} A/m^2, and (b) current density j.

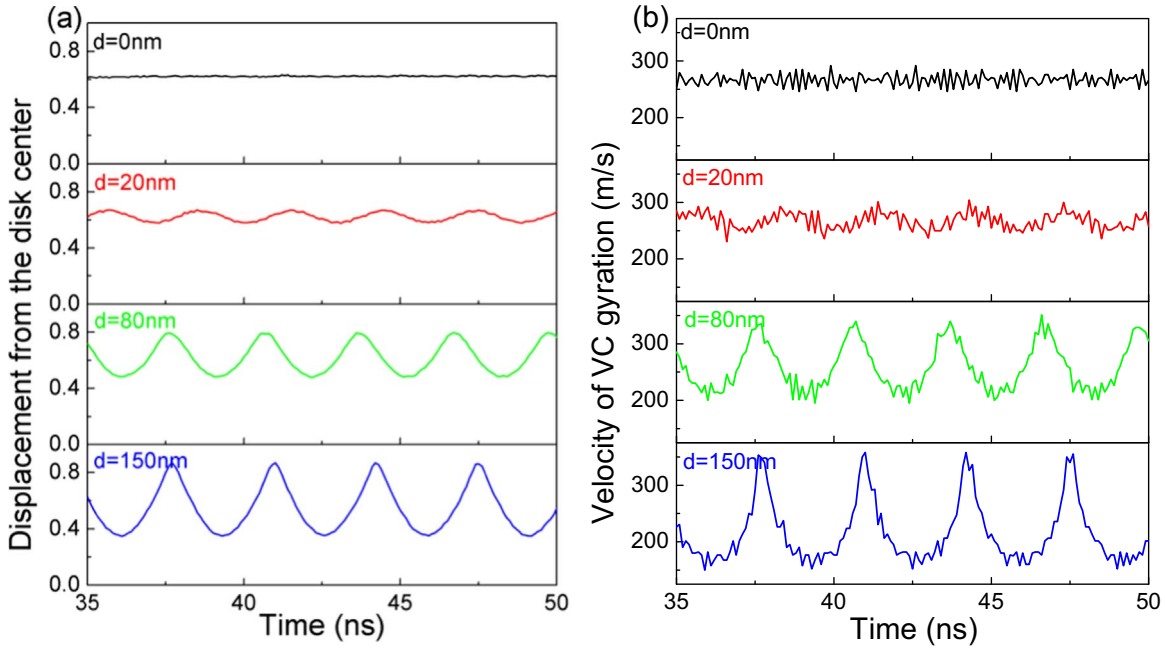

Fig. 6. (a) Displacement from the disk center as a function of time on the steady orbits. (b) Velocity of VC gyration as a function of time on the steady orbits, where j=8×10^{11} A/m^2.

periodic changes of velocity will be advantageous to control the polarity switching and other dynamical behaviors of vortex.

Finally, in order to make a concise expression about the discussion above and to gain a more in-depth understanding of the vortex oscillation, we plot the steady trajectory for d=80 nm and d=150 nm in Fig. 7, where the positions of velocity peaks are symbolized with red dots, and the backgrounds show the contour plots of the Oersted field energy versus the VC position. It is observed that the peaks of velocity always appear at relative concentrated positions on the orbits, meaning the VC moves very quickly at lower Oersted field energy region. Actually, we have deeply analyzed the physical origin of velocity periodic fluctuation [40] and found that the periodical fluctuation of gyrotropic frequency, together with the periodical changes of displacements from the disk center, results in the concentrating appearances of the velocity peaks on the trajectory. Comparing total effective potential energy shown in the background of Fig. 2 with Oersted field energy shown in the background of Fig. 7, we find that the Oersted field energy is dominant in the system total energy, and it is the main reason that influences the shape of the VC trajectory.

3. Conclusion

In summary, the magnetic vortex dynamics driven by spin-polarized current is investigated in an off-centered nanocontact structure through micromagnetic simulations. In contrast to the usual single nanocontact structure in which the circular symmetry of total effective energy with difficulty to trigger the magnetic vortex and the uniform gyrotropic frequency of the steady oscillation, we demonstrate that the symmetry of total potential energy is broken in such off-centered nanocontact geometry, leading to the magnetic vortex is easier to be triggered and reliable controllability of vortex gyration, including trajectory, eigenfrequency, excitation time and instantaneous velocity. Simultaneously, the simulations show that it is possible to utilize the nanocontact position to change the total effective potential energy of the system so as to realize the pinning of the vortex core.

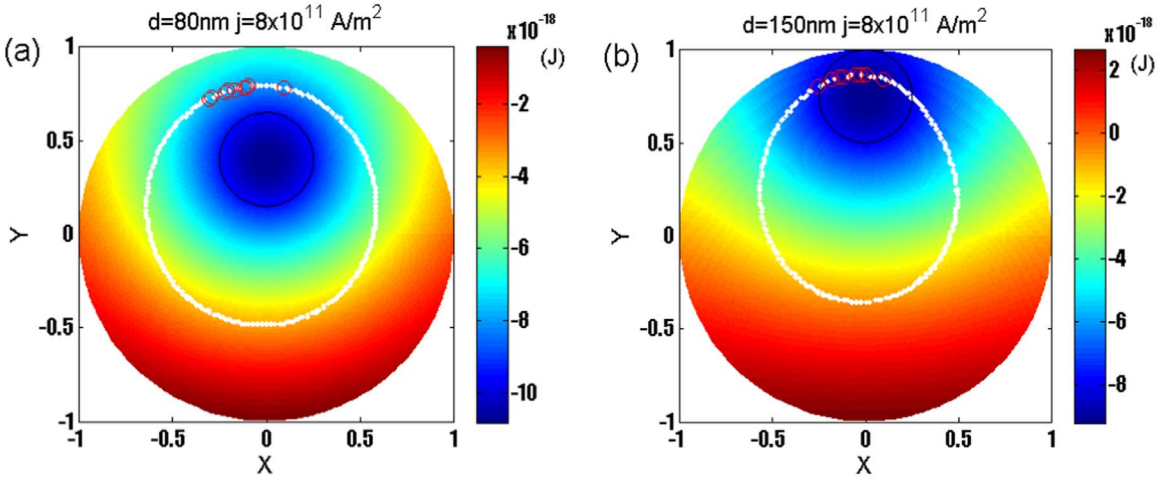

Fig. 7. The steady trajectory of VC (white dots) with the backgrounds showing the contour plots of the Oersted field energy, where the red circles represent the positions where the instantaneous velocity peaks appear and the black circle denotes the nanocontact.

Acknowledgments

This work was supported by China Postdoctoral Science Foundation (Grant no. 2013M541286), Science and Technology Planning Project of Jilin Province (Grant nos. 20140520109JH and 20150414003GH) and "Twelfth Five-year" Scientific and Technological Research Project of Department of Education of Jilin Province (Grant no. 2015-211).

Appendix A. Supplementary material

Supplementary data associated with this article can be found in the online version at doi:10.1016/j.ssc.2016.12.015.

References

[1] K.Yu Guslienko, Nat. Nanotechnol. 8 (2008) 2745.
[2] T. Shinjo, T. Okuno, R. Hassdorf, Science 289 (2000) 930.
[3] J. Stöhr, H.C. Siegmann, Magnetism: From Fundamentals to Nanoscale Dynamics, Springer Verlag, Berlin Heidelberg, 2006.
[4] V. Novosad, F.Y. Fradin, P.E. Roy, K.S. Buchanan, K.Yu Guslienko, S.D. Bader, Phys. Rev. B 72 (2005) 024455.
[5] X. Zhu, Z. Liu, V. Metlushko, P. Grutter, M.R. Freeman, Phys. Rev. B 71 (2005) 180408.
[6] K.Yu Guslienko, W. Scholz, R.W. Chantrell, N. Novosad, Phys. Rev. B 71 (2005) 144407.
[7] G. Consolo, L. Lopez-Diaz, L. Torres, G. Finocchio, A. Romeo, B. Azzerboni, Appl. Phys. Lett. 91 (2007) 162506.
[8] A. Puzic, B.Van Waeyenberge, K.W. Chou, P. Fischer, T. Tyliszczak, K. Rott, H. Bruckl, G. Reiss, I. Neudecker, T. Haug, M. Buess, C.H. Back, J. Appl. Phys. 97 (2005), 2005, p. 10E704.
[9] V.S. Pribiag, I.N. Krivorotov, G.D. Fuchs, P.M. Braganca, O. Ozatay, J.C. Sankey, D.C. Ralph, R.A. Buhrman, Nat. Phys. 3 (2007) 498.
[10] B.A. Ivanov, C.E. Zaspel, Phys. Rev. Lett. 99 (2007) 247208.
[11] Y. Liu, H. He, Z. Zhang, Appl. Phys. Lett. 91 (2007) 242501.
[12] A.V. Khvalkovskiy, J. Grollier, A. Dussaux, K.A. Zvezdin, V. Cros, Phys. Rev. B 80 (2009) 140401 (R).
[13] R. Lehndorff, D.E. Bürgler, S. Gilga, R. Hertel, P. Grünberg, C.M. Schneider, Z. Celinski, Phys. Rev. B 80 (2009) 054412.
[14] Y.S. Choi, K.S. Lee, S.K. Kim, Phys. Rev. B 79 (2009) 184424.
[15] G. Finocchio, V.S. Pribiag, L. Torres, R.A. Buhrman, B. Azzerboni, Appl. Phys. Lett. 96 (2010) 102508.
[16] M. Carpentieri, L. Torres, J. Appl. Phys. 107 (2010) 073907.
[17] A.A. Awad, A. Lara, V. Metlushko, K.Yu Guslienko, F.G. Aliev, Appl. Phys. Lett. 100 (2012) 262406.
[18] X.W. Yu, V.S. Pribiag, Y. Acremann, A.A. Tulapurkar, T. Tyliszczak, K.W. Chou, B. Braüer, Z.P. Li, O.J. Lee, P.G. Gowtham, D.C. Ralph, R.A. Buhrman, J. Stöhr, Phys. Rev. Lett. 106 (2011) 167202.
[19] Q. Mistral, M. van. Kampen, G. Hrkac, J.V. Kim, T. Devolder, P. Crozat, C. Chappert, L. Lagae, T. Schrefl, Phys. Rev. Lett. 100 (2008) 257201.
[20] M. Manfrini, T. Devolder, J.V. Kim, P. Crozat, N. Zerounian, C. Chappert, W.Van Roy, L. Lagae, G. Hrkac, T. Schrefl, Appl. Phys. Lett. 95 (2009) 192507.
[21] D.V. Berkov, N.L. Gorn, Phys. Rev. B 80 (2009) 064409.
[22] T. Devolder, J.V. Kim, P. Crozat, C. Chappert, M. Manfrini, M. van. Kampen, W. VanRoy, L. Lagae, G. Hrkac, T. Schrefl, Appl. Phys. Lett. 95 (2009) 012507.
[23] E. Jaromirska, L. Lopez-Diaz, A. Ruotolo, J. Grollier, V. Cros, D. Berkov, Phys. Rev. B 83 (2011) 094419.
[24] S. Petit-Watelot, J.V. Kim, A. Ruotolo, R.M. Otxoa, K. Bouzehouane, J. Grollier, A. Vansteenkiste, B.V. deWilele, V. Cros, T. Devolder, Nat. Phys. 8 (2012) 682.
[25] V. Sluka, A. Kákay, A.M. Deac, D.E. Bürgler, R. Hertel, C.M. Schneider, Phys. Rev. B 86 (2012) 214422.
[26] G.E. Rowlands, I.N. Krivorotov, Phys. Rev. B 86 (2012) 094425.
[27] M.W. Keller, A.B. Kos, T.J. Silva, W.H. Rippard, M.R. Pufall, Appl. Phys. Lett. 94 (2009) 193105.
[28] S. Kasai, Y. Nakatani, K. Kobayashi, H. Kohno, T. Ono, Phys. Rev. Lett. 97 (2006) 107204.
[29] A.V. Khvalkovskiy, J. Grollier, N. Locatelli, Ya.V. Gorbunov, K.A. Zvezdin, V. Cros, Appl. Phys. Lett. 96 (2010) 212507.
[30] G. Finocchio, O. Ozatay, L. Torres, R.A. Buhrman, D.C. Ralph, B. Azzerboni, Phys. Rev. B 78 (2008) 174408.
[31] G.R. Aranda, J.M. Gonzalez, J.J. del V, K.Yu Guslienko, J. Appl. Phys. 108 (2010) 123914.
[32] Y.S. Choi, M.W. Yoo, K.S. Lee, Y.S. Yu, H. Jung, S.K. Kim, Appl. Phys. Lett. 96 (2010) 072507.
[33] Y. Liu, H.N. Li, Y. Hu, A. Du, J. Appl. Phys. 112 (2012) 093905.
[34] Y. Liu, H.N. Li, Y. Hu, A. Du, Solid. State Commun. 193 (2014) 61.
[35] H.N. Li, Y. Liu, M. Jia, A. Du, Chin. Phys. B. 24 (4) (2015) 047501.
[36] S.R. Sani, J. Persson, S.M. Mohseni, V. Fallahi, J. Akerman, J. Appl. Phys. 109 (2011) 07C913.
[37] S. Kaka, M.R. Pufall, W.H. Rippard, T.J. Silva, S.E. Russek, J.A. Katine, Nature 437 (2005) 389.
[38] J.C. Slonczewski, J. Magn. Magn. Mater. 159 (1996) L1.
[39] M.J. Donahue, D.G. Porter, OOMMF User's Guide, Version 1.2a5 available online: ⟨http://math.nist.gov/oommf/⟩
[40] H.N. Li, Y. Liu, M. Jia, A. Du, J. Magn. Magn. Mater. 386 (2015) 8.
[41] Y. Liu, M. Jia, H.N. Li, Y. Hu, A. Du, J. Magn. Magn. Mater. 401 (2016) 124.
[42] Y.S. Choi, S.K. Kim, K.S. Lee, Y.S. Yu, Appl. Phys. Lett. 93 (2008) 182508.